Bragg-Type Resonance in Blocked Pipe System and Its Effect on the Eigenfrequency Shift

Moez Louati[1]; Mohamed S. Ghidaoui, M.ASCE[2]; Silvia Meniconi[3]; and Bruno Brunone, M.ASCE[4]

Abstract: Recent studies of measured transient pressure signals showed that eigenfrequencies shift with changes in cross-sectional area of the conduit and used this fact to develop blockage-detection algorithms. However, an understanding of the physical basis for eigenfrequency shift-based algorithms is currently lacking. This paper shows heuristically, analytically, and numerically that a blockage in either unbounded or bounded pipe systems interacts strongly with waves at specific frequencies. These specific interacting frequencies conform precisely to Bragg's resonance condition. The frequency interval between consecutive Bragg frequencies is proportional to the wave speed divided by the blockage length. In addition, it is found that pipe blockage imposes a distinct signature through Bragg resonance phenomena on the unbounded and bounded pipe systems in exactly the same manner (i.e., they exhibit the same variation pattern). It is further shown that the eigenfrequency shift, currently used without physical basis or explanation in many published papers as a basis for blockage detection methods, is because of the Bragg resonance effect. Examples are used to show how this physical insight into the nature and cause of the eigenfrequency shifts can be advantageously used to design direct blockage detection techniques. **DOI: 10.1061/(ASCE)HY.1943-7900.0001383.**

Author keywords: Bragg resonance; Blockage; Eigenfrequency shift; Pipe system; Transient wave.

Introduction

Analytical, numerical and experimental studies of measured transient pressure signals show that system eigenfrequencies vary with the cross-sectional area of the conduit (e.g., Duan et al. 2011; Qunli and Fricke 1990; Domis 1980; Schroeder 1967; Mermelstein 1967). This observation was instrumental in developing blockage-detection algorithms using inverse formulations to link measured eigenfrequencies with cross-sectional area (or degree of blockage) of the pipe (e.g., Duan et al. 2011, 2013; Stephens 2008; De Salis and Oldham 1999; Schroeter and Sondhi 1994; Qunli and Fricke 1990; Domis 1980; Mermelstein 1967; Schroeder 1967).

The use of eigenfrequency shift to detect blockages is promising and has led to proof of concept under idealized laboratory settings, but there are several unresolved issues. Foremost is the fact that the physical basis for this wave-blockage interaction is currently not known or understood.

This paper studies the forward problem so that a direct explanation for the mechanism responsible for the observed eigenfrequency shifts in the presence of a blockage in a bounded pipe system can be sought. Once the physical basis for the forward problem is established and adequately understood, one may hope to address the challenging computational issues that arise in connection with its inversion and solution. The foundational relationship between wave-blockage interactions and eigenfrequency shift is investigated in two steps.

First, this work considers an unbounded pipe system with changes in the cross-sectional area. This permits (1) direct examination of the interactions between waves and blockage without interference from other effects or reflections from boundaries; and (2) an investigation of those wave frequencies that minimally propagate (transmit) through a blockage section. Conversely, one may examine without external influences those waves that are maximally reflected back toward the source (Louati 2013). Understanding the reasons for maximal wave transmission and maximum wave reflection provides insight into the coupling mechanism between the upstream and downstream regions of the blockage. It will be seen that these insights are useful in the design of effective probing signals. For example, Duan et al. (2015) swept the frequency bandwidth (FBW) of the probing signal to obtain the highest reflection coefficient that leads to accurate detectability of the blockage. It will be shown heuristically, analytically, and theoretically that this mechanism is directly related to Bragg resonance effects (Bragg and Bragg 1913).

The second step considers a blockage in a bounded pipe system [e.g., a reservoir-pipe-valve (RPV) system] and relates wave transmission and reflection (Bragg resonance) to the observed variations in system eigenfrequencies. Finally, some implications of Bragg resonance phenomena for practical blockage detection are discussed at the end of the paper.

Heuristic Approach

Before providing analytical and numerical details, it is useful to preface any discussion of the complex interaction between waves

[1]Postdoctoral Fellow, Dept. of Civil and Environmental Engineering/School of Engineering, Hong Kong Univ. of Science and Technology, Kowloon, Hong Kong (corresponding author). E-mail: mlouati@connect.ust.hk

[2]Chair Professor, Dept. of Civil and Environmental Engineering/School of Engineering, Hong Kong Univ. of Science and Technology, Kowloon, Hong Kong. E-mail: ghidaoui@ust.hk

[3]Assistant Professor, Dept. of Civil and Environmental Engineering, Univ. of Perugia, 06125 Perugia, Italy. E-mail: silvia.meniconi@unipg.it

[4]Professor, Dept. of Civil and Environmental Engineering, Univ. of Perugia, 06125 Perugia, Italy. E-mail: bruno.brunone@unipg.it

Note. This manuscript was submitted on September 13, 2016; approved on June 8, 2017; published online on October 27, 2017. Discussion period open until March 27, 2018; separate discussions must be submitted for individual papers. This paper is part of the ***Journal of Hydraulic Engineering***, © ASCE, ISSN 0733-9429.

and conduit nonuniformities by introducing the reader to the Bragg resonance condition (Bragg and Bragg 1913).

Bragg and Bragg (1913) introduced a mathematical condition to explain why crystals, at certain specific wavelengths and incident angles, produced intense peaks of reflected radiation. Bragg and Bragg (father and son) received a Nobel prize for this work, and their derived condition is now called Bragg's law or Bragg resonance. It is widely found to apply in many fields of engineering and science. In hydraulics, Mei (1985) applied Bragg's condition to explain resonant reflection of surface waves by periodic sandbars. To date, however, Bragg resonance phenomena have not been studied in water supply pipelines.

To see how Bragg's condition arises in transient waves in pipes, consider a train of incident monochromatic waves with wavelength, λ, propagating from the right end toward the left (Fig. 1). These waves reflect partially from Junctions 1 and 2. Seen from the incident waves, there is a reduction in cross-sectional area at Junctions 1 and 2, and, therefore, Junctions 1 and 2 preserve the sign of the incident wave. The wave reflected from Junction 2 propagates a distance $2\ l_2$ more than the wave reflecting from Junction 1. Because both waves are positive, the waves reflecting from Junctions 1 and 2 experience constructive interference when the $n\lambda = 2l_2$ and destructive interference when $(2n+1)\lambda/2 = 2l_2$, where $n = 1,2,3, \ldots$ This is precisely Bragg's resonance condition. When $n\lambda = 2l_2$ (called Bragg's resonance or condition of maximum reflection), the reflected wave acquires maximum amplitude because of constructive interference. Conversely, when $(2n+1)\lambda/2 = 2l_2$ (called Bragg's resonance or condition of total transmission), the reflected wave acquires minimum amplitude because of destructive interference; thus, the transmitted wave is maximum.

Next, Bragg resonance for an unbounded pipe (Fig. 2) is considered. The main difference between the systems in Figs. 1 and 2 is that Junction 2 of the latter is an increase in diameter and, therefore, changes the sign of the incident wave (i.e., a positive wave is reflected as negative and vice versa). Consequently, the waves reflecting from Junction 1 and Junction 2 experience constructive interference when $(2n+1)\lambda/2 = 2l_2$ and destructive interference when $n\lambda = 2l_2$ where $n = 1,2,3, \ldots$ That is, Bragg's resonance (condition of maximum reflection) is $(2n+1)\lambda/2 = 2l_2$, and Bragg's resonance or condition of maximum transmission is $n\lambda = 2l_2$. Notice that Bragg's resonance condition is thus related also to the length of the blockage. Thus, for Bragg resonance to occur, the incident wavelength must be short enough to be close to $4l_2$.

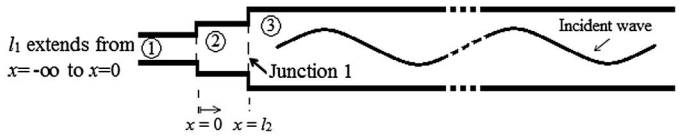

Fig. 1. Sketch of a pipe system with nonuniformities

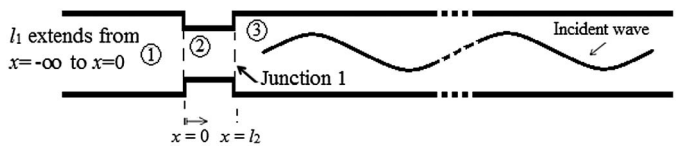

Fig. 2. Pipe system with one blockage

Analytical Approach

The mathematical foundation of the heuristic approach described in the last section is provided here. Consider a wave train generated by a hydrophone, a hydraulic device, or an acoustic transmitter that propagates in pipe 3 toward Junction 1 in Fig. 1 or 2. Suppose that this incident wave train has a wave number, k, and an angular frequency, w, and amplitude p_0. Its form is $p_0 \exp(ikx - iwt)$ with $i = \sqrt{-1}$. This wave field is governed by the water hammer equations (Ghidaoui 2004). Classical water hammer equation for a frictionless pipe using the coupling of continuity and momentum equations (e.g., Chaudhry 2014; Ghidaoui 2004) is considered here.

Realizing that water supply systems are low Mach number flows, the classical water hammer equation in a frictionless pipe has the following form (Ghidaoui 2004)

$$\frac{\partial^2 P}{\partial t^2} = \frac{a^2}{A}\frac{\partial}{\partial x}\left(A\frac{\partial P}{\partial x}\right) \tag{1}$$

where a = acoustic wave speed; and $A(x)$ and A_0 = cross sectional area of the conduit in both the nonuniform and uniform region, respectively. The low Mach number assumption is justified because typical flow velocities in water supply systems are of the order of 1 m/s, whereas the wave speed is of the order of 1,000 m/s; thus, the Mach number is of the order 0.001.

Using the method of separation of variables, the solution to Eq. (1) is of the form $p(x,w)\ \exp(-iwt)$, where w and $p(x,w)$ are the radian frequency and the amplitude of the propagating wave in the pipe, respectively. Noting that the cross-section A varies from pipe to pipe but is constant for each pipe section, Eq. (1) for each pipe "j" (=1, 2, 3) (Figs. 1 and 2) becomes

$$\frac{d^2 p_j}{dx} + k_j^2 p_j = 0 \tag{2}$$

where $k_j = w/a$ = wave-number of the jth pipe segment. For simplicity but without loss of generality, the wave speed a is assumed to be the same for all segments. The solution of Eq. (2) is

$$p_j = p_j^{\text{ref}} \exp(ik_j x) + p_j^{tr} \exp(-ik_j x) \tag{3}$$

where p_j^{tr} and p_j^{ref} = transmitted and reflected wave amplitudes in pipe j, respectively.

In this case, $j = 1$ is the pipe section to the left of Junction 2; $j = 2$ is the pipe section between Junctions 1 and 2 (which may be thought of as a blockage in Fig. 2); and $j = 3$ is the pipe section to the right of Junction 1. The conditions of pressure and flow continuity at the Junction of segments j and $j+1$ (i.e., junctions 1 and 2) are

$$\begin{cases} p_j = p_{j+1} \\ A_j \dfrac{dp_j}{dx} = A_{j+1}\dfrac{dp_{j+1}}{dx} \end{cases} \quad \text{at} \quad x = -l_{j+1} + \sum_1^j l_{j+1}; \quad \text{where } j = 1,2,3, \ldots \tag{4}$$

where A_j and l_j = area and length of the jth pipe. Eqs. (3) and (4) can be solved for any number of blockages. For simplicity, only the case of single blockage (Fig. 2) is discussed in this work. The extension to multiblockages is algebraically involved but can be performed using software packages such as *MATLAB*. The case of periodic multiblockages is considered in Louati (2013). Assuming no reflections from the upstream and downstream boundaries and an amplitude of the incident wave p_0 (i.e., $p_1^{\text{ref}} = 0$ and $p_3^{tr} = p_0$), Eqs. (3) and (4) give

$$\begin{cases} \dfrac{p_3^{\text{ref}}}{p_0} = \dfrac{2(1-\alpha^2)[(1+\alpha^2)\sin^2(kl_2) + 2i\alpha\cos(kl_2)\sin(kl_2)]}{2(1+\alpha^4)\sin^2(kl_2) + 4\alpha(\cos^2(kl_2)+1)} \\ \dfrac{p_1^{tr}}{p_0} = \dfrac{1}{\cos(kl_2) + i\frac{1+\alpha^2}{2\alpha}\sin(kl_2)} \end{cases} \tag{5}$$

where

$$\alpha = A_2/A_0 \tag{6}$$

Minimum transmission occurs when the norm of p_1^{tr} is normalized by p_0

$$\left|\frac{p_1^{tr}}{p_0}\right|^2 = \frac{1}{\cos^2(kl_2) + \left[\frac{1+\alpha^2}{2\alpha}\right]^2 \sin^2(kl_2)} \tag{7}$$

is minimum. Minimization of Eq. (7) gives

$$\cos(kl_2) = 0 \Rightarrow w_n^R(l_2) = 2\pi\left[(2n-1)\frac{a}{4l_2}\right]; \qquad n = 1, 2, 3 \tag{8}$$

which provides the frequencies (wavelengths) of the source at which minimum transmission (i.e., maximum reflection) occurs. This is precisely the condition that was arrived at heuristically in the previous section and is the Bragg's resonance or condition of maximum reflection.

Maximization of Eq. (7) gives

$$\sin(kl_2) = 0 \Rightarrow w_n^T(l_2) = 2\pi\left[2(n-1)\frac{a}{4l_2}\right]; \qquad n = 1, 2, 3 \tag{9}$$

which provides the frequencies (wavelengths) of the source at which maximum transmission occurs. As in the previous case, this is precisely the Bragg's resonance or condition of maximum transmission.

Eq. (8) indicates that if the blockage length is an odd multiple of the quarter wavelength, then maximum wave reflection from a blockage occurs. On the other hand, Eq. (9) indicates that if the blockage length is a multiple of the half wavelength, then the injected wave is totally transmitted through the blockage. For example, Duan et al. (2015) used a blockage detection technique that relies on measuring the reflection coefficient. In the experimental work, Duan et al. (2015) varied the central frequency of the generated wave to determine which wave frequencies reflect maximally, which results in maximum reflection (and accuracy) according to the Bragg resonance condition. In the experiments, Duan et al. (2015) found that for blockage lengths equal to odd integer multiples of the quarter wavelength, the power reflection ratio becomes maximum. Again, this is precisely the condition of Bragg resonance frequency of maximum reflection [Eq. (8)].

Figs. 3 and 4 show the variation of transmitted, p_1^{tr}, and reflected amplitude, p_3^{ref}, with respect to the frequency (w) for two different blockage lengths l_2 (=3.6 and 24 m), respectively. Moreover, to investigate the effect of the blockage radial extent, $\alpha = 0.64$, $\alpha = 0.36$, and $\alpha = 0.16$ are considered in Figs. 3(a–c) and 4(a–c), respectively.

To improve readability and visual comparison of the graphs in Figs. 3 and 4, the dimensionless amplitude and frequency are presented by dividing p_1^{tr} and p_3^{ref} by the incident wave amplitude, p_0, and w by $w_1^R(l_2 = 24\text{ m})$ defined by

$$w_1^R(l_2) = 2\pi\frac{a}{4l_2} \tag{10}$$

obtained from Eq. (8) for $n = 1$.

The existence of Bragg-type resonance, in which there are frequency bands exhibiting full transmission and others exhibiting (near) complete reflection is clearly seen in Figs. 3 and 4 and occurs for all α. This implies that occurrence of Bragg resonance depends

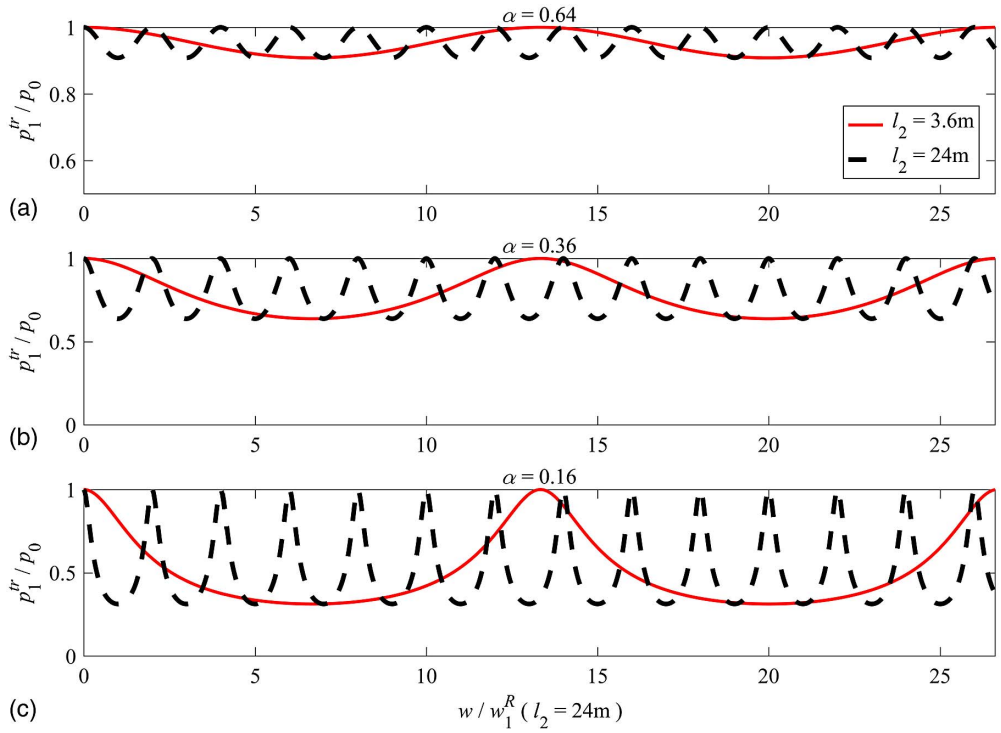

Fig. 3. Transmission amplitude variation with frequency: (a) $\alpha = 0.64$; (b) $\alpha = 0.36$; (c) $\alpha = 0.16$

J. Hydraul. Eng., 2018, 144(1): 04017056

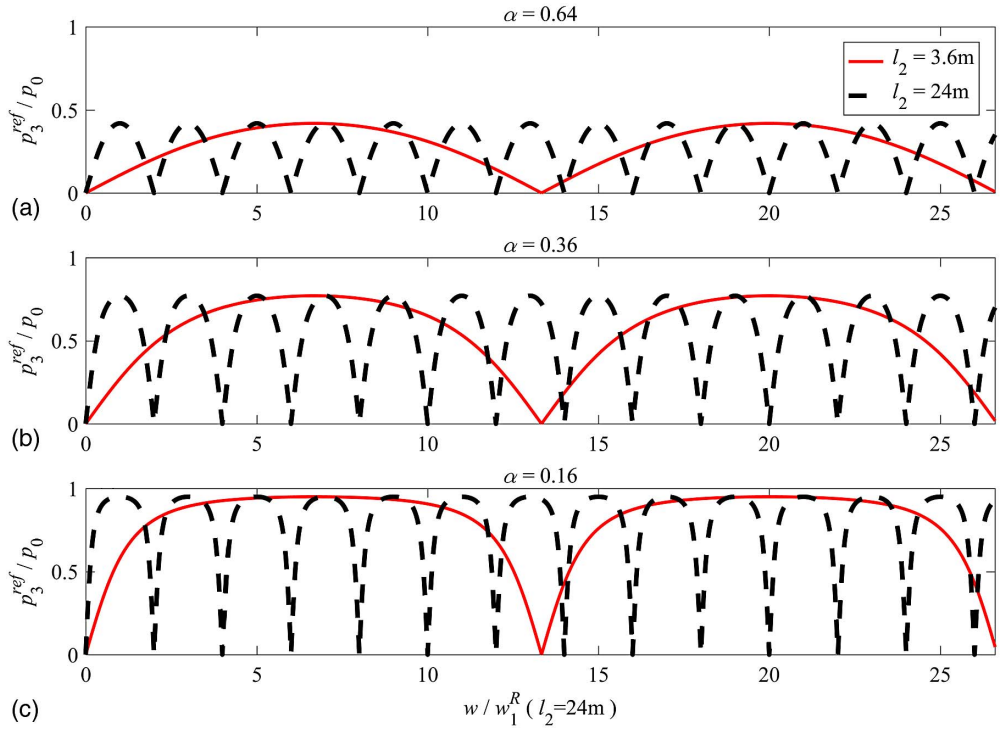

Fig. 4. Reflection amplitude variation with frequency: (a) $\alpha = 0.64$; (b) $\alpha = 0.36$; (c) $\alpha = 0.16$

on pipe and blockage length scale but not on its radial scale. However, the radial scale does affect the severity of Bragg resonance (see amplitude variation for different α in Figs. 3 and 4). The frequencies at which maximum reflection and maximum transmission occur correspond to Eqs. (8) and (9), respectively. The near-complete reflection is because of multiple wave reflections from the Junction boundaries of the blockage. For instance, consider the wave impinging on the blockage in Region 2 (Fig. 2), upon reaching Junction 1, part of the incident wave is reflected, and part is transmitted. The transmitted part of the wave propagates to the left and splits into a reflected part and a transmitted part upon reaching Junction 2. The reflected part is split into reflected and transmitted wave components upon reaching Junction 1. The transmitted part, having the same phase as the impinging wave, resonates with the incident wave in Region 3 (Fig. 2).

The smallest frequency for which an incident wave experiences maximum reflection toward the source (i.e., minimum transmission through the blockage) is given by Eq. (10). That is, an incident wave whose wavelength is $4l_2$ interacts with the blockage in such a way that maximum reflection toward the wave source occurs. An analogous result is found in shallow water waves propagating in a channel that contains a shelf (Mei 1985). Eqs. (8) and (9) may be physically understood as follows. Consider a train of waves generated at the source (Fig. 2). Any wave in this train arriving at the blockage ($x = l_2$) experiences scattering, whereby a part of the incident wave is reflected back toward the source, and a part is transmitted toward the other end of the blockage ($x = 0$). Once the transmitted part of the wave arrives at $x = 0$, it becomes scattered such that a part of the incident wave is reflected toward $x = l_2$. The result is that each wave in the train experiences multiple scattering at the two ends of the blockage $x = l_2$ and $x = 0$ and, thus, interacts with waves both ahead of it and after it in the wave train.

Waves with frequencies given by Eq. (9) exhibit destructive interference at $x = l_2$, whereas waves with frequencies given by Eq. (8) exhibit constructive interference at $x = l_2$. It is precisely this type of interaction that transient-based defect detection methods (TBDDM) exploit to identify defects. For example, measuring the frequency spectrum of p_1^{tr} (Fig. 3) allows the identification of the system blockage properties. The blockage length is determined by reading the lowest frequency at which the amplitude of the spectrum is minimum and plugging this value into the left-hand side of Eq. (10). The radial extent of the blockage is inferred by reading the height of the first minimum of the frequency spectrum of p_1^{tr}, then plugging it into Eq. (7) and keeping the physically meaningful solution for which $\alpha < 1$. The result is

$$\alpha = \left|\frac{p_0}{p_1^{tr}(w_1^R)}\right| - \sqrt{\left(\left|\frac{p_0}{p_1^{tr}(w_1^R)}\right| - 1\right)} \tag{11}$$

Figs. 3 and 4 show that longer blockage (extended blockage) leads to narrower frequency bands of Bragg resonance. Moreover, Figs. 3 and 4 show that the maximum reflection and transmission amplitudes depend on the radial extent α and that these amplitudes increase with severity of blockage (as α decreases). For severe short blockage cases, Figs. 3(c) and 4(c) show that the frequency bands of maximum reflection become wider than the frequency bands for maximum transmission. This means that severe short blockage (e.g., a malfunctioning valve slightly open) reflects most of the waves and allows only narrow frequency bands to transmit through. In other words, the likelihood of Bragg resonance occurrence is higher as the blockage becomes more severe. These features are discussed in more depth in the section on bounded pipe systems. Practical implications of Bragg resonance are discussed toward the end of the paper.

Numerical Investigation

Numerical tests are conducted using the method of characteristic (MOC) (Chaudhry 2014) to study the interaction of wave

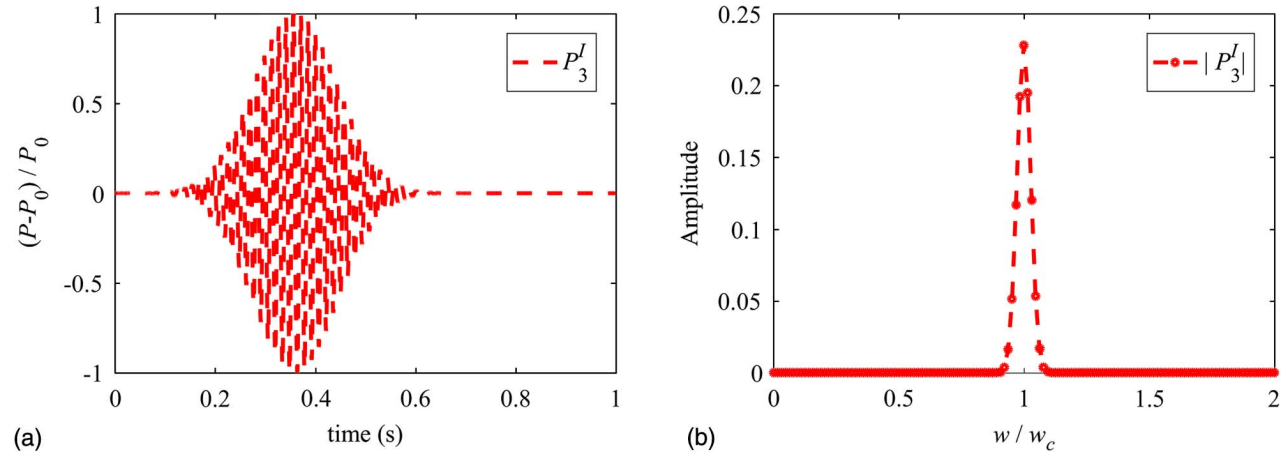

Fig. 5. Input signal as transient source for numerical investigation

reflections and transmissions in an unbounded pipe system with a blockage of length $l_2 = 3.6$ and $\alpha = 0.16$. The waveform of the incident wave in Region 3 (Fig. 2) is given by

$$\begin{cases} P_3^I(t) = p_0 \exp\left(-4\dfrac{w_c^2}{\beta^2}\log(10)\left(t-\dfrac{\beta}{w_c}\right)^2\right)\sin\left(w_c\left(t-\dfrac{\beta}{w_c}\right)\right) \\ \text{where } 0 < t \le t_{\text{wave}} = \dfrac{\beta}{w_c} \text{ with } \beta = 100\pi \end{cases} \tag{12}$$

where w_c = central frequency; and β = coefficient that controls the FBW. Fig. 5 shows both time and frequency domains of the generated waveform. This particular waveform is chosen because it limits the FBW and the central frequency generated. As shown in Fig. 5, a very narrow FBW is considered to study waves of approximately single frequency. TFlow in the pipe is initially zero. P_3^I and P_3^R, respectively, denote the incident and reflected pressure waves in Region 3, and P_1 is the pressure wave in Region 1.

Fig. 6 shows the time and frequency domains of the pressure signal at Regions 1 and 3 in which the central frequency of the generated wave is $w_c = w_1^R$ [Eq. (8)]. Maximum reflection is expected to occur at $w = w_1^R$. Indeed, Fig. 6(a) shows that most of the wave energy is reflected as seen in Fig. 6(c). In fact, Fig. 6(b) shows that the amplitude of the reflected wave is of the order of the initially generated wave; conversely, Fig. 6(d) shows the amplitude of the transmitted wave is much smaller.

Fig. 7 shows the case in which the central frequency is $w_c = w_2^T = 2w_1^R$ [Eq. (9)]. In this case, maximum transmission is expected to occur. Figs. 7(a–d) show that the amplitude of the reflected wave (P_3^R) is much smaller than the transmitted wave (P_1). Fig. 7(b) shows that the wave propagating at exactly w_2^T is totally transmitted as expected from Fig. 3.

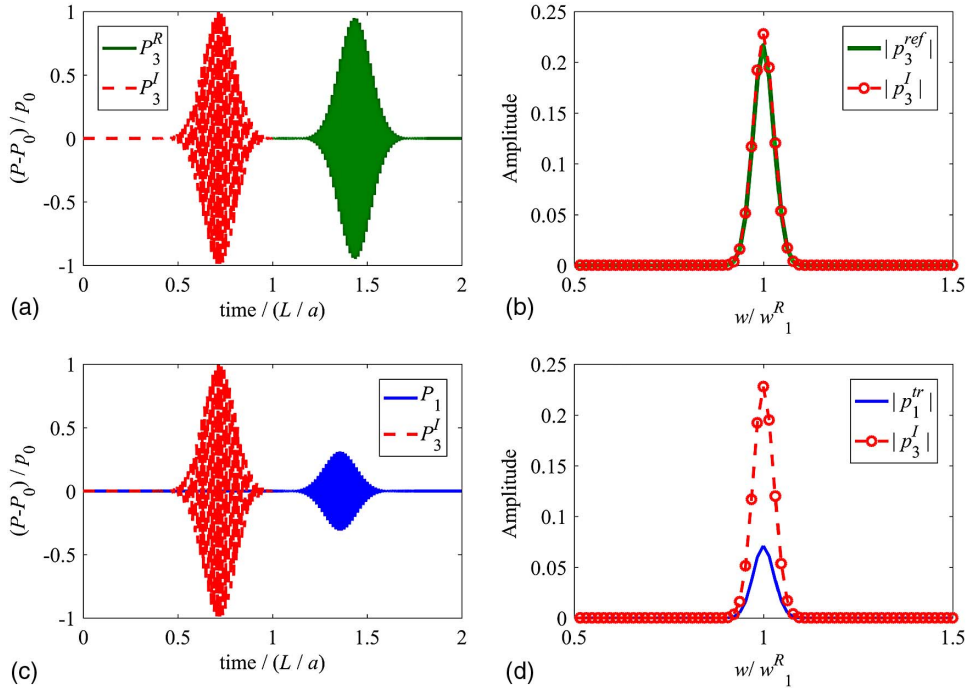

Fig. 6. Pressure measurement in Region 1 (upstream) and Region 3 (downstream) of the blocked pipe system (Fig. 2) when $w_c = w_1^R$ [Eq. (8)]

J. Hydraul. Eng., 2018, 144(1): 04017056

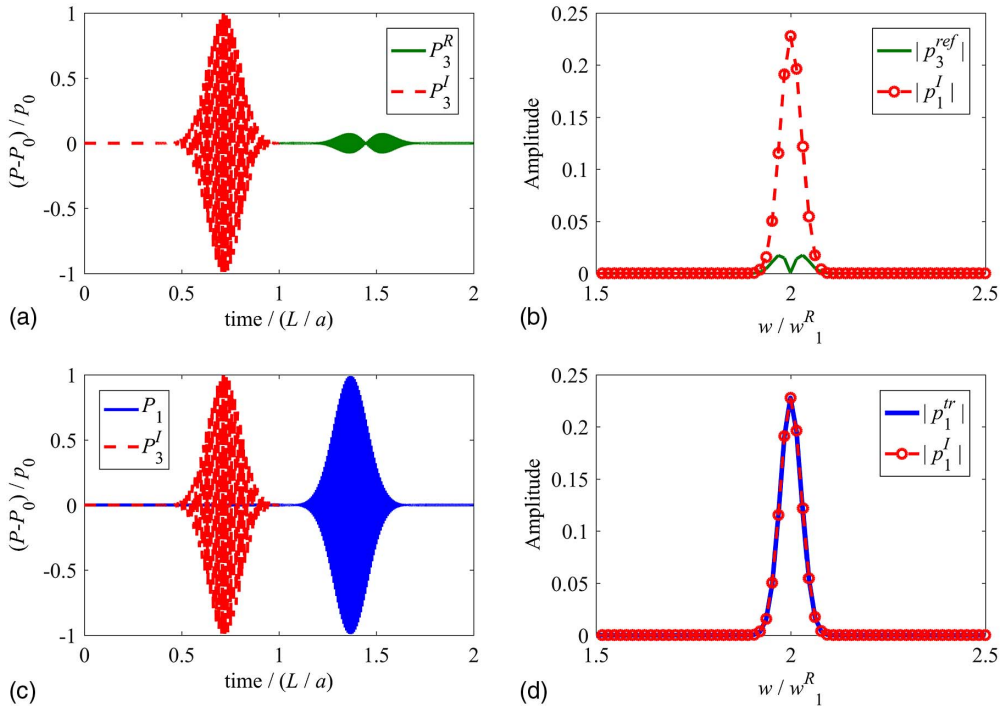

Fig. 7. Pressure measurement in Region 1 (upstream) and Region 3 (downstream) of the blocked pipe system (Fig. 2) when $w_c = w_2^T$ [Eq. (9)]

The results in Figs. 6 and 7 show the occurrence of Bragg resonance when the Bragg's conditions [Eqs. (8) and (9)] are satisfied.

Wave-Blockage Interaction in a Bounded Pipe and Bragg Resonance

For an intact (i.e., defect free) reservoir-pipe-valve (RPV) system with pipe length L, the eigenfrequencies (natural resonant frequencies) are given by the following dispersion relation (Chaudhry 2014)

$$\cos(k_m^0 L) = 0 \Rightarrow w_m^0 = a k_m^0 = 2\pi\left[(2\,m-1)\frac{a}{4L}\right]; \quad m = 1, 2, 3\ldots \tag{13}$$

where $k_m^0 = w_m^0/a$ = mth wave number; w_m^0 = mth eigenfrequency; and the superscript "0" denote *intact case*. For a RPV system with a single blockage as shown in Fig. 8, the eigenfrequencies are governed by the following dispersion relation (El-Rahed and Wagner 1982; Duan et al. 2011)

$$\begin{aligned}&\alpha\cos(k_m l_1)\cos(k_m l_2)\cos(k_m l_3)\\ &-\cos(k_m l_1)\sin(k_m l_2)\sin(k_m l_3)\\ &-\alpha^2\sin(k_m l_1)\sin(k_m l_2)\cos(k_m l_3)\\ &-\alpha\sin(k_m l_1)\cos(k_m l_2)\sin(k_m l_3) = 0\end{aligned} \tag{14}$$

where the subscript m = mth natural resonant mode; and $k_m = w_m/a$ = mth wave number, where w_m = mth eigenfrequency; and a = acoustic wave speed. The blocked pipe system in Fig. 8 is modeled as the Junction of three pipes in series with different diameters (Fig. 8). The three pipes are defined as pipe 1 with length l_1 and cross-sectional area $A_1 = A_0$; pipe 2 with length l_2 and cross-sectional area $A_2 < A_0$; and pipe 3 with length l_3 and cross-sectional area $A_3 = A_0$, where A_0 is the intact cross-sectional area. The ratio between the cross-sectional areas is $\alpha = A_2/A_0$, and

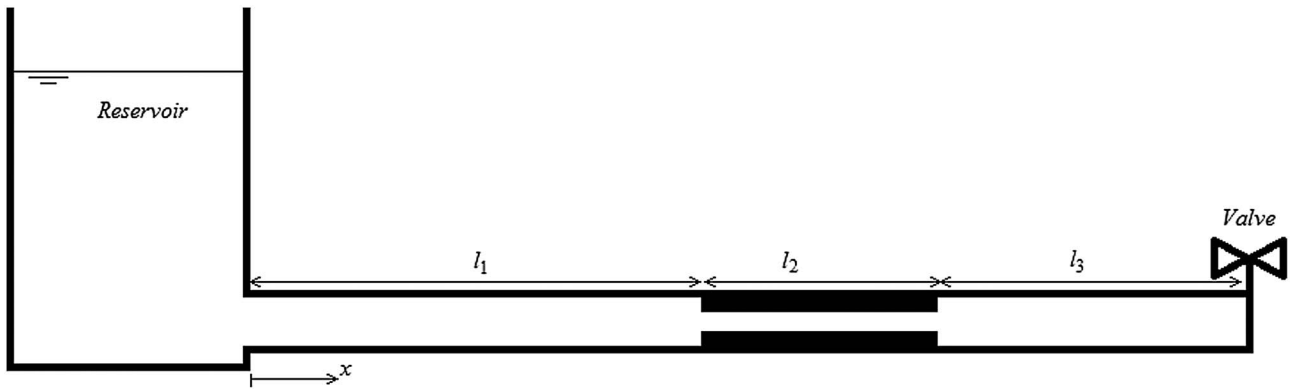

Fig. 8. A single blockage in a reservoir-pipe-valve system (bounded system)

the dimensionless lengths are defined by x/L, $\eta_1 = l_1/L$, $\eta_2 = l_2/L$ and $\eta_3 = l_3/L$, where $L = l_1 + l_2 + l_3$ = total length of the blocked pipe system, and x = distance along the pipe length from the reservoir (Fig. 8). The pipe flow is assumed one dimensional and frictionless. When $\alpha = 1$, Eq. (14) becomes identical to the dispersion relation of the *intact pipe case* in Eq. (13).

It is interesting and important to note that Bragg's resonance conditions [Eqs. (8) and (9)], derived for the unbounded pipe system, could be imposed on the dispersion relation Eq. (14) to show the effect of Bragg resonance on the eigenfrequency shift. Inserting Eq. (9) into Eq. (14) gives

$$\alpha \cos(w_n^T l_2/a)[\cos(w_n^T l_1/a)\cos(w_n^T l_3/a) - \sin(w_n^T l_1/a)\sin(w_n^T l_3/a)] = 0 \quad (15)$$

which leads to

$$\cos(w_n^T(l_1 + l_3)/a)\cos(w_n^T l_2/a) = 0 \quad (16)$$

Considering the following manipulation, which uses Bragg's condition of maximum transmission [$\sin(w_n^T l_2/a) = 0$]:

$$\cos(w_n^T(l_1 + l_3)/a)\cos(w_n^T l_2/a) - \underbrace{\sin(w_n^T l_2/a)\cos(w_n^T(l_1 + l_3)/a)}_{=0} = 0 \quad (17)$$

yields

$$\cos(w_n^T L/a) = 0 \quad (18)$$

which is the dispersion relation for intact pipe case [Eq. (13)] at $w_m = w_n^T$. That is, at Bragg's condition of maximum transmission, the wave passes through the blockage unaffected, and the blocked pipe system behaves as if it were intact.

Similarly, inserting Eq. (8) into Eq. (14) gives

$$\sin(w_n^R l_2/a)[\alpha^2 \sin(w_n^R l_1/a)\cos(w_n^R l_3/a) + \cos(w_n^R l_1/a)\sin(w_n^R l_3/a)] = 0 \quad (19)$$

which leads to

$$\alpha^2 \sin(w_n^R l_1/a)\cos(w_n^R l_3/a) + \cos(w_n^R l_1/a)\sin(w_n^R l_3/a) = 0 \quad (20)$$

Eq. (20) corresponds to the dispersion relation of either a reservoir-pipe-reservoir (RPR) system with length $(l_1 + l_3)$ having a blockage at the downstream boundary with a blockage length l_3 and an area ratio $\bar{\alpha} = \alpha^2$, as shown in Fig. 9(a); or a valve-pipe-valve (VPV) system with length $(l_1 + l_3)$ having a blockage at the upstream boundary with a blockage length l_1 and an area ratio $\bar{\alpha} = \alpha^2$, as shown in Fig. 9(b). This means that at modes with eigenfrequencies equal or close to the Bragg resonance frequency of maximum reflection ($w_m = w_n^R$), the eigenfrequency shift behaves similarly to the shift in a blocked pipe system with a blockage at the boundary with squared area ratio (Fig. 9). The eigenfrequency shift mechanism for such simple blocked pipe system with a blockage at the boundary is well studied and understood in previous work by Louati and Ghidaoui (2016).

To test the findings of the effect of Bragg's resonance conditions on the eigenfrequency behavior, the following two blockage cases are studied: ($\eta_2 = 0.15$, $\alpha = 0.16$) and ($\eta_2 = 0.027$, $\alpha = 0.16$). The eigenfrequencies of the blocked pipe system are obtained using Eq. (14), and the results are plotted in Figs. 10 and 11. These figures show the eigenfrequency (w_m) variation with length

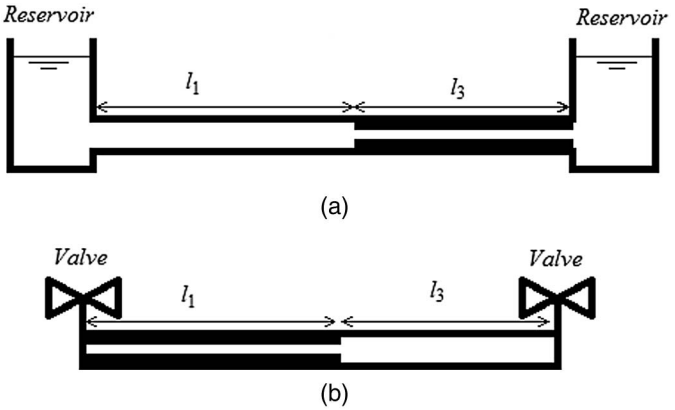

Fig. 9. Equivalent blocked pipe system with length $(l_1 + l_3)$ and dimensionless blocked area α^2 corresponding to the dispersion relation in Eq. (20); (a) RPR system with a blockage of length l_3 at the downstream boundary; (b) VPV system with a blockage of length l_1 at the upstream boundary

$\eta_b = \eta_3 + 0.5\eta_2$ for the first 15 and 40 modes for $\eta_2 = 0.15$ and $\eta_2 = 0.027$, respectively. The eigenfrequencies of the intact pipe case ($\alpha = 1$) are the straight horizontal lines in Figs. 10 and 11. Clearly, the presence of the blockage causes an eigenfrequency shift of most but not all modes. The nonshifted eigenfrequencies correspond to Bragg resonance frequencies of maximum transmission [Eq. (9)]. For example, Figs. 10 and 11 show that the eigenfrequencies of the blocked and intact pipe system are the same for w_m/w_1^0 around 13 and 27 for ($\eta_2 = 0.15$) and around 74 for ($\eta_2 = 0.027$). These are precisely the Bragg's resonance of maximum transmission. To verify this, for the blockage case with length $\eta_2 = 0.15$, the Bragg's resonance condition of maximum transmission requires $w_m l_2/a = m\pi$. This gives $w_m/w_1^0 = 2m/\eta_2 = 2m/0.15 = 13.33m$ = (13.33, 26.66, ...), which agree with the values in Fig. 10. For the blockage case with length $\eta_2 = 0.027$, the Bragg's resonance condition of maximum transmission gives $w_m/w_1^0 = 2m/\eta_2 = 2m/0.027 = 74.07m$ = (74.07, ...), which agrees with the value in Fig. 11(b).

In addition, Figs. 10 and 11 show that, at modes $m = 4$ (i.e., $2m - 1 = 7$) and $m = 11$ (i.e., $2m - 1 = 21$) for $\eta_2 = 0.15$; and $m = 19$ ($2m - 1 = 37$) for $\eta_2 = 0.027$, the eigenfrequency shift has regular variation with equal positive and negative shift magnitude variations. This shift behavior is similar to the shift behavior for the case of blocked pipe system with a blockage at the boundary (Louati and Ghidaoui 2016). In fact, in Figs. 12(a and b) and 13, the eigenfrequency shift at modes $m = 4$ (i.e., $2m - 1 = 7$) and $m = 11$ (i.e., $2m - 1 = 21$) for $\eta_2 = 0.15$, and $m = 19$ ($2m - 1 = 37$) for $\eta_2 = 0.027$, are compared with the eigenfrequency shift of a blocked RPR system with blockage at the downstream boundary [Fig. 9(a)]. The results show good agreement between both blocked pipe systems when the blockage area ratio in RPR is $\alpha = (0.16)^2$. The eigenfrequencies at these modes correspond very closely the Bragg resonance frequencies of maximum reflection. To verify this, for the blockage case with length $\eta_2 = 0.15$, the Bragg's resonance condition of maximum reflection requires $w_m l_2/a = (2m - 1)\pi/2$. This gives $w_m/w_1^0 = (2m - 1)/0.15 = 6.66(2m - 1)$ = (6.66, 20, ...), which agree with the values in Fig. 10. For the blockage case with length $\eta_2 = 0.027$, the Bragg's resonance condition of maximum reflection gives $w_m/w_1^0 = (2m - 1)/0.027 = 37.03(2m - 1)$ = (37.03, ...), which agrees with the value in Fig. 11. Although not shown here, similar results were found for different α values.

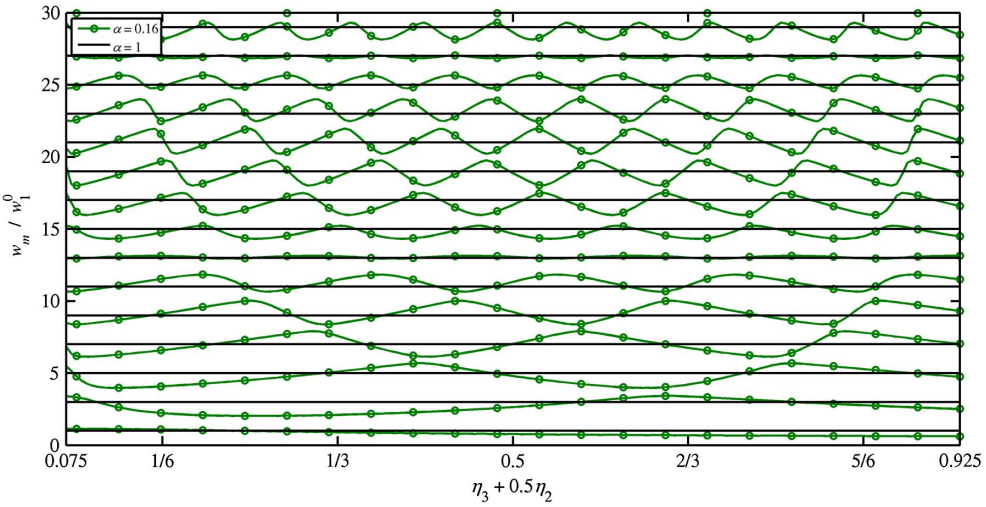

Fig. 10. Normalized eigenfrequency variation with length $\eta_b = \eta_3 + 0.5\eta_2$ of the first 15 modes when $\alpha = 0.16$ and $\eta_2 = 0.15$ along with the asymptotic solutions

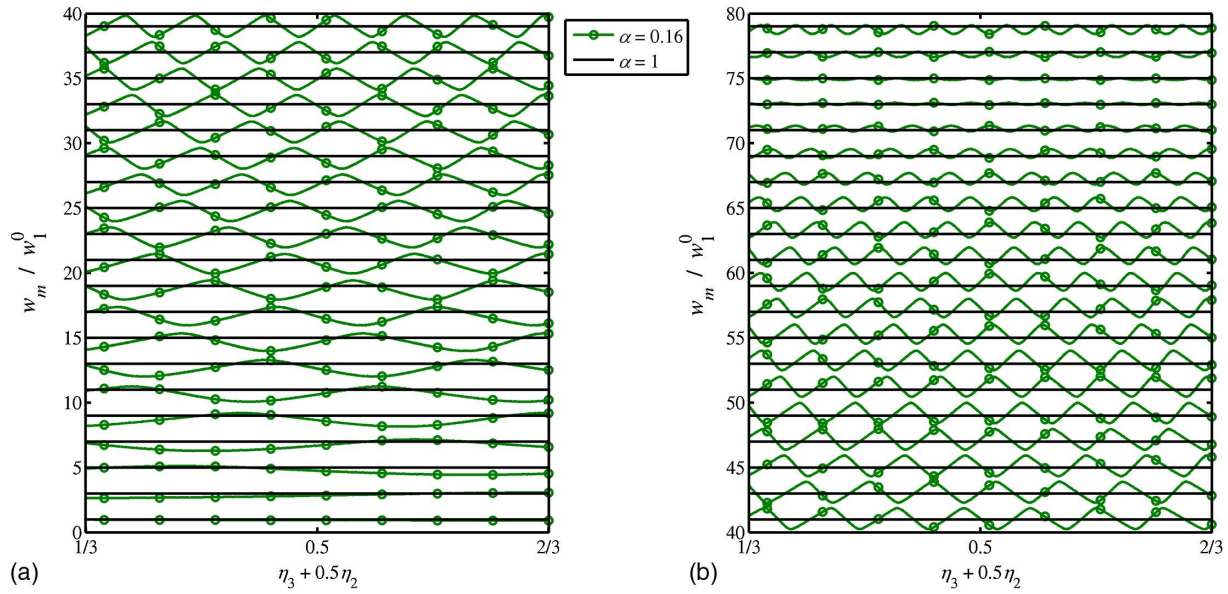

Fig. 11. Normalized eigenfrequency variation with length $\eta_b = \eta_3 + 0.5\eta_2$ when $\alpha = 0.16$ and $\eta_2 = 0.027$ along with the asymptotic solutions for (a) the first 20 modes; (b) modes $m = 21$ to $m = 40$

Does Bragg Resonance Arise in Practice?

Bragg resonance and its effects in closed-conduit flows are neither emphasized nor directly addressed in previous water supply research. This lack of reference to the Bragg phenomena does not mean that Bragg resonance and its effects do not occur. The fact that eigenfrequency shifts are observed in experiments and are recorded and discussed in the literature (Meniconi et al. 2013; Stevens 2000) makes clear that Bragg resonance is important. This work clearly shows that Bragg resonance governs the magnitude and sign of these observed eigenfrequency shifts. However, Bragg resonance is less likely to be observed in real pipe systems for two primary reasons, as discussed in the following paragraphs.

First, it is clear in Figs. 3(a) and 4(a) that at low frequency $[w/w_1^R(l_2) < 0.2]$, the Bragg resonance effect is weak. This is important because most transient waves arising in practice are relatively low frequency: (1) *deliberately generated transient waves* are slowly executed (that is, the length of pipe traversed by the wavefront in the time taken to complete the control action) maneuvers such as pump start-up or shutdown, and thus are quite low frequency; (2) *accidental transient waves* such as those generated by a pump failure or improper maneuver of a valve are also of relatively low frequency because of the small inertia of these devices; and (3) *probing transient waves* for defect detection (e.g., Brunone et al. 2014) are also generated at low frequency. It is, therefore, not surprising that significant effects of Bragg resonance are not evident in systems responses at these low wave frequencies.

For example, in defect detection practice, probing transient waves are usually generated by mechanical devices (e.g., manual valve closure or intentional pump stops) with closure times of a few seconds. For example, with a typical wave speed for nonplastic

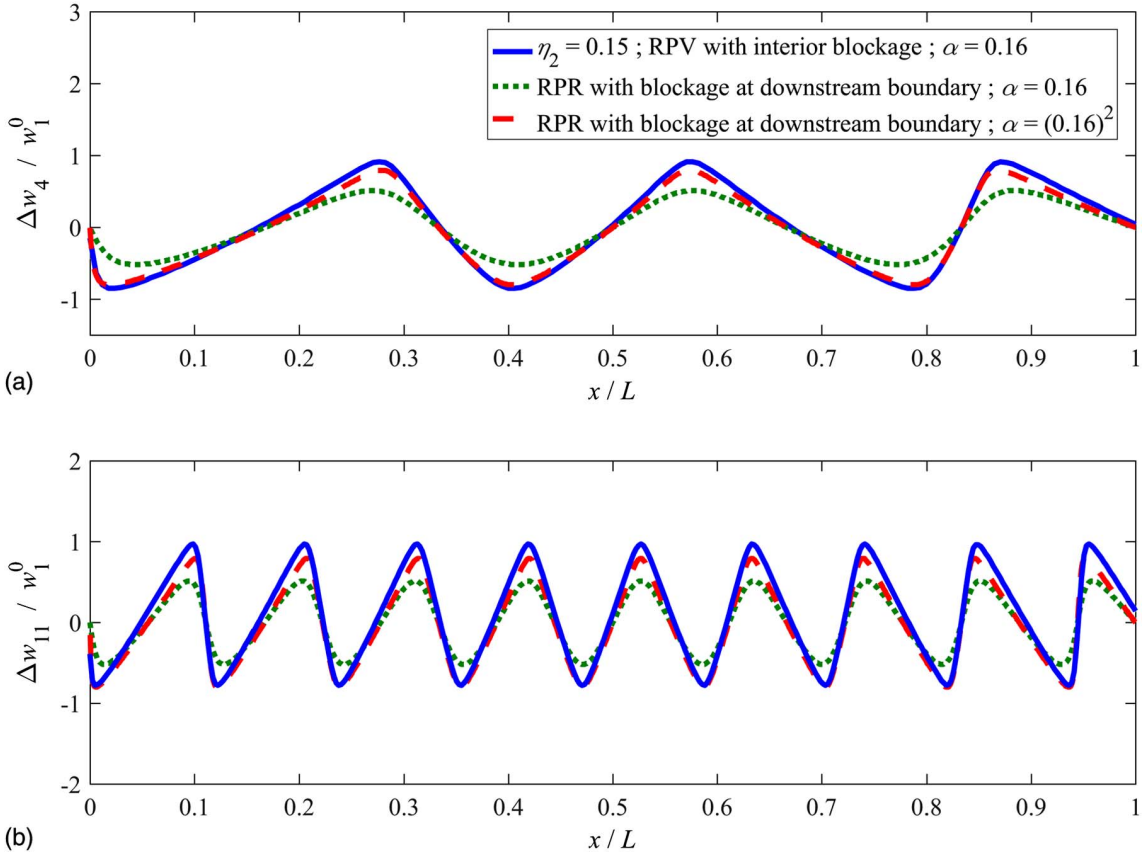

Fig. 12. Comparison of eigenfrequency shifts of blocked RPV system with interior blockage (for $\eta_2 = 0.15$) and RPR system with blockage at the boundary; (a) at mode $m = 4$ (i.e., $2m - 1 = 7$); (b) at mode $m = 11$ (i.e., $2m - 1 = 21$)

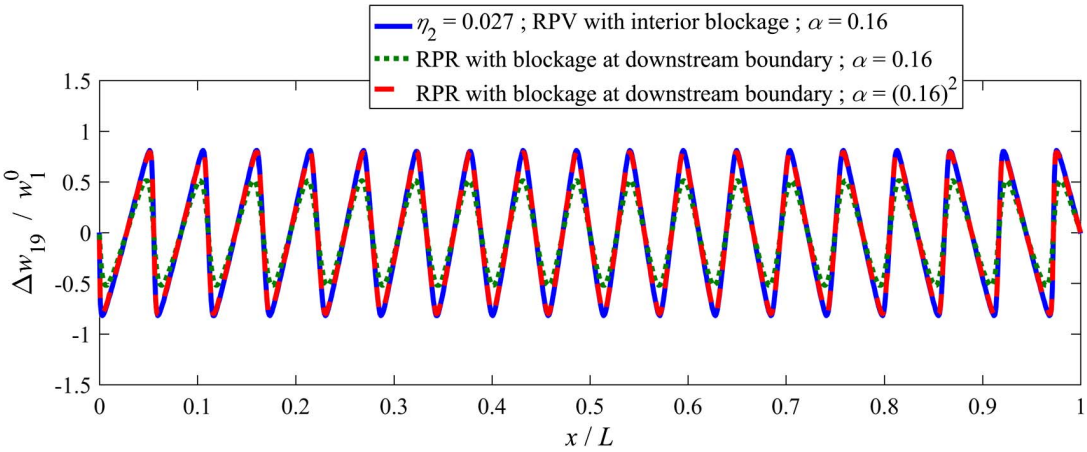

Fig. 13. Comparison of eigenfrequency shifts of blocked RPV system with interior blockage (for $\eta_2 = 0.027$) and RPR system with blockage at the boundary at mode $m = 19$ (i.e., $2m - 1 = 37$)

pipes in water systems of circa 1,000 m/s, the generated wavelength for a 5-s maneuver (wave-generating action) is around $\lambda \approx 5{,}000$ m. Therefore, Bragg resonance would only be expected to occur (and be potentially detectable) for blockages with lengths around $l_2 = \lambda/4 = 1{,}250$ m [Eq. (10)] or longer. Recently, faster maneuvers are being used to generate probing transient waves (e.g., use of fast solenoid valves) with closure times as low as 50 ms to increase the accuracy of transient-based defect detection methods (e.g., Meniconi et al. 2011). In this case, Bragg resonance could occur with blockages as short as $l_2 = \lambda/4 = 12.5$ m. In another paper (Louati et al. 2017), the authors conducted experimental laboratory tests to study and demonstrate the effect of Bragg resonance in a blocked pipe system.

Second, in real systems, blockages may be multiple with variable sizes (e.g., severe random roughness). In this case, the effects of Bragg resonance could become weaker, because when an incident wave of a given wavelength encounters random blockages, some blockages with lengths satisfying Bragg's condition of maximum reflection would enhance reflection of the wave, whereas others with lengths satisfying Bragg's condition of maximum

transmission would have the opposite effect. Thus, the effect of Bragg resonance may be averaged out (Lu et al. 2011).

Implications of Bragg Resonance to Blockage Detection in Pipes

It is logical that stronger interactions between a wave and a blockage give clearer indications of the presence of the blockage. For cases with stronger Bragg resonance effects, eigenfrequency shifts may provide better indicators of pipe blockage in terms of both magnitude and location. Thus, identifying Bragg resonance frequencies and their effects is important in developing transient defect detection algorithms, including blockage and leaks. Ongoing work in other papers submitted by the authors describes in more detail the techniques being developed to identify Bragg resonance frequencies from the frequency response function and how Bragg resonance phenomena could be used for blockage detection. Note that the previous sections of this paper show that the frequency interval between consecutive Bragg resonance frequencies are proportional to the ratio of wave speed to blockage length. Hence, a wide FBW produced by the probing transient generator is required to capture the signature of a short blockage (i.e., a discrete blockage with length less than 2 m). This is pointed out in previous work by the authors (e.g., Louati and Ghidaoui 2015; Lee et al. 2014). For example, for a blockage with length 1 m and a pipe system wave speed of 1,000 m/s, the frequency interval between two consecutive Bragg frequencies is of the order of 1 kHz; accordingly, the injected signal must have a FBW of the order of several kHz. Injection of such wide bandwidth signals cannot be accomplished by current, mechanical, wave-generator technology such as valves. In fact, the current work is part of a research project (http://smartuws.ust.hk/) that aims to make use of high-frequency (≫kHz) acoustic waves for defect detection in water supply pipelines.

Another interesting feature of Bragg resonance is that its effects are also related to the characteristics of the blockage (i.e., blockage length and area), a fact that may also be useful for blockage identification. For example, the Bragg resonance frequency of maximum reflection (w_1^R) is a function of the blockage length [Eq. (10)]. If w_1^R is identified, then the blockage length can be determined by $l_2 = 2\pi a/(4w_1^R)$. Moreover, if maximum shift is measured at the Bragg resonance of maximum reflection, then the blockage area ratio (α) could be determined using the simplified blockage model located at a boundary (Louati and Ghidaoui 2016). This is possible because Eq. (20) shows that, at a resonant mode with eigenfrequency near or equal to the Bragg resonance frequency of maximum reflection, the blocked pipe system (Fig. 8) behaves like a simplified pipe system with blockage at the boundary (Fig. 9).

Conclusions

This work constitutes a first step in understanding how wave-blockage interaction (i.e., Bragg resonance) relates to the variation in observed eigenfrequency shifts for a simple, blocked pipe system. This is done in two stages. First, the transmission and reflection of injected pressure waves in unbounded pipe containing a blockage are studied, which allows the direct examination of interactions between waves and blockage sections without interference from other effects (boundaries) and the investigation of which waves transmit least, and conversely which waves reflect most toward the source (Bragg resonance). Second, the knowledge of which waves transmit and which do not is used to study and understand the mechanism of eigenfrequency shift induced by a blockage in a bounded pipe system. It is found that the variation of maximum shift magnitudes at different resonant modes is related to the Bragg resonance frequencies. The key conclusions are summarized as follows:

1. If the blockage length is a multiple of the half wavelength, then the injected wave is totally transmitted through the blockage. The frequencies of such waves are called Bragg resonance frequencies of total transmission (w_n^T). On the other hand, if the blockage length is an odd multiple of the quarter wavelength, then maximum wave reflection from the blockage occurs. The frequencies of these waves are called Bragg resonance frequencies of maximum reflection (w_n^R).
2. A zero or nearly zero eigenfrequency shift occurs at modes with eigenfrequencies equal or close to the Bragg resonance frequencies of total transmission (w_n^T). This is because at $w_m = w_n^T$, total transmission occurs, and, therefore, the blocked pipe system behaves as an intact pipe system.
3. Maximum eigenfrequency shift occurs at modes with eigenfrequencies equal or close to the Bragg resonance frequencies of maximum reflection (w_n^R). This is because at $w_m = w_n^R$, the blockage reflects most of the impinging waves, and, therefore, the blockage effect is enhanced.
4. At modes with eigenfrequencies equal or close to the Bragg resonance frequency of maximum reflection ($w_m = w_n^R$), the eigenfrequency shift behaves similarly to the shift in a blocked pipe system with a blockage at the boundary with squared area ratio. The eigenfrequency shift mechanism for this simple blocked pipe system with a blockage at the boundary is well studied and understood in previous work (Louati and Ghidaoui 2016).
5. The smaller the blockage length is, the smaller the eigenfrequency shifts are at low modes. This is because, for short (discrete) blockages, the Bragg resonant frequencies occur only at high-resonant modes (high frequencies). Therefore, if an injected FBW contains only lower frequencies, the blockage signature is reduced and may become unclear. The FBW should be either large enough or should sweep a large enough frequency range to include frequencies close to the Bragg resonance frequency of maximum reflection. However, short blockages with large radial protrusion induce large Bragg resonance FBW of maximum reflection, which increases the shift at lower modes.
6. For small blockages (e.g., $\eta_2 = 0.027$ in Fig. 11), the Bragg resonant frequencies [Eqs. (8) and (9)] could be at very high-resonant modes (high frequencies), and the transient flow plane wave assumption (for a one-dimensional model) may no longer be valid. If such high frequencies are to be used, then the behavior of high-frequency (dispersive and nonplane) waves needs to be investigated. The authors have studied this subject in another paper.
7. Some practical implications of Bragg resonance effects are discussed. In particular, Bragg's condition is directly related to the characteristics of blockages; therefore, knowledge of the Bragg resonance frequencies provides information on the blockage size.

Acknowledgments

This study is supported by the Hong Kong Research Grant Council (projects 612712 & 612713 & T21-602/15R), by the Postgraduate Studentship, the University of Perugia, the Italian Ministry of Education, University and Research (MIUR)—under the Projects of Relevant National Interest "Advanced analysis tools for the

management of water losses in urban aqueducts" and "Tools and procedures for an advanced and sustainable management of water distribution systems"—and Fondazione Cassa Risparmio Perugia, under the project "Hydraulic and microbiological combined approach toward water quality control (No. 2015.0383.021)". The authors thank Dr. D. A. McInnis for the technical and editorial suggestions.

Notation

The following symbols are used in this paper:

A = acoustic wave speed in water (ms^{-1});
A_0 = area of intact pipe (m^2);
A_2 = area of pipe 2 (the blocked region in the pipe) (m^2);
$i = \sqrt{-1}$;
j = pipe number;
k = wave number (m^{-1});
L = whole pipe length (m);
l_1 = length of pipe 1 (m);
l_2 = length of pipe 2 (m);
l_3 = length of pipe 3 (m);
l_j = length of pipe $j = 1,2$ or 3 (m);
m = resonant mode number for pipe system of length L;
m_1 = mode number for subsystem 1;
m_2 = mode number for subsystem 2;
$P(x,t)$ = pressure (Pa);
P_0 = initial pressure in the pipe (Pa);
$p(x,w)$ = amplitude of the harmonic pressure (Pa);
p_0 = maximum pressure amplitude injected at the source (Pa);
p_j^{ref} = reflected pressure amplitude at pipe region j (Pa);
p_j^{tr} = transmitted pressure amplitude at pipe region j (Pa);
t = time (s);
w = angular frequency (rad s^{-1});
w_m = mth resonant frequencies in the blocked pipe case (rad s^{-1});
w_m^0 = mth resonant frequencies in the intact pipe case (rad s^{-1});
w_m^s = mth resonant frequencies in the shallow blockage case (rad s^{-1});
w_n^R = Bragg resonance frequency of maximum reflection (rad s^{-1});
w_m^T = Bragg resonance frequency of maximum reflection (rad s^{-1});
x = axial coordinate (m);
α = area ratio between A_2 and A_0;
Δw_m = mth eigenfrequency shift;
$\eta_j = l_j/L$ dimensionless length;
η_2^0 = zero shift blockage positions; and
λ = probing wave length (m).

References

Bragg, W. H., and Bragg, W. L. (1913). "The reflection of X-rays by crystals." *Proc. R. Soc. London Ser. A.*, 88(605), 428–438.

Brunone, B., et al. (2014). "The characterization of Milan WDS by pumping switching off: Field test assessment." *Procedia Eng.*, 70, 201–208.

Chaudhry, M. H. (2014). *Applied hydraulic transients*, 3rd Ed., Springer, New York.

De Salis, M. H. F., and Oldham, D. J. (1999). "Determination of blockage area function of a finite duct from a single pressure response measurement." *J. Sound Vib.*, 221(1), 180–186.

Domis, M. A. (1980). "Frequency dependence of acoustic resonances on blockage position in a fast reactor subassembly wrapper." *J. Sound Vib.*, 72(4), 443–450.

Duan, H., Lee, P. J., Ghidaoui, M. S., and Tung, Y. (2011). "Extended blockage detection in pipelines by using the system frequency response analysis." *J. Water Resour. Plann. Manage.*, 10.1061/(ASCE)WR.1943-5452.0000145, 55–62.

Duan, H., Lee, P. J., Kashima, A., Lu, J., Ghidaoui, M., and Tung, Y. (2013). "Extended blockage detection in pipes using the system frequency response: Analytical analysis and experimental verification." *J. Hydraul. Eng.*, 10.1061/(ASCE)HY.1943-7900.0000736, 763–771.

Duan, W., Kirby, R., Prisutova, J., and Horoshenkov, K. V. (2015). "On the use of power reflection ratio and phase change to determine the geometry of a blockage in a pipe." *Appl. Acoust.*, 87, 190–197.

El-Rahed, M., and Wagner, P. (1982). "Acoustic propagation in rigid ducts with blockage." *J. Acoust. Soc. Am.*, 72(3), 1046–1055.

Ghidaoui, M. S. (2004). "On the fundamental equations of water hammer." *Urban Water J.*, 1(2), 71–83.

Lee, P. J., Duan, H., Tuck, J., and Ghidaoui, M. (2014). "Numerical and experimental study on the effect of signal bandwidth on pipe assessment using fluid transients." *J. Hydraul. Eng.*, 10.1061/(ASCE)HY.1943-7900.0000961, 04014074.

Louati, M. (2013). "On wave-defect interaction in pressurized conduits." *Proc., 35th IAHR Congress*, International Association for Hydro-Environment Engineering and Research, Madrid, Spain.

Louati, M., and Ghidaoui, M. S. (2015). "Wave-blockage interaction in pipes." *Proc., 36th IAHR Congress*, International Association for Hydro-Environment Engineering and Research, Madrid, Spain.

Louati, M., and Ghidaoui, M. S. (2016). "In-depth study of the eigenfrequency shift mechanism due to variation in the cross-sectional area of a conduit." *J. Hydraul. Res.*, in press.

Louati, M., Meniconi, M., Ghidaoui, M. S., and Brunone, B. (2017). "Experimental study of the eigenfrequency shift mechanism in blocked pipe system." *J. Hydraul. Eng.*, 10.1061/(ASCE)HY.1943-7900.0001347, 04017044.

Lu, J., Koliskins, A., Ghidaoui, M. S., and Duan, H. (2011). "The effect of random inhomogeneities on wave propagation in pipes." *Proc., 34th IAHR Congress*, International Association for Hydro-Environment Engineering and Research, Madrid, Spain.

MATLAB [Computer software]. MathWorks, Natick, MA.

Mei, C. C. (1985). "Resonant reflection of surface waves by periodic sandbars." *J. Fluid Mech.*, 152(1), 315–335.

Meniconi, S., Brunone, B., Ferrante, M., and Massari, C. (2011). "Small amplitude sharp pressure waves to diagnose pipe systems." *Water Resour. Manage.*, 25(1), 79–96.

Meniconi, S., Duan, H., Lee, P., Brunone, B., Ghidaoui, M., and Ferrante, M. (2013). "Experimental investigation of coupled frequency and time-domain transient test-based techniques for partial blockage detection in pipelines." *J. Hydraul. Eng.*, 10.1061/(ASCE)HY.1943-7900.0000768, 1033–1040.

Mermelstein, P. (1967). "Determination of the vocal-tract shape from measured formant frequencies." *J. Acoust. Soc. Am.*, 41(5), 1283–1294.

Qunli, W., and Fricke, F. (1990). "Determination of blocking locations and cross-sectional area in a duct by eigenfrequency shifts." *J. Acoust. Soc. Am.*, 87(1), 67–75.

Schroeder, M. R. (1967). "Determination of the geometry of the human vocal tract by acoustic measurements." *J. Acoust. Soc. Am.*, 41(4B), 1002–1010.

Schroeter, J., and Sondhi, M. M. (1994). "Techniques for estimating vocal-tract shapes from the speech signal." *IEEE Trans. Speech Audio Process.*, 2(1), 133–150.

Stephens, M. (2008). "Transient response analysis for fault detection and pipeline wall condition assessment in field water transmission and distribution pipelines and networks." Ph.D. thesis, Univ. of Adelaide, Adelaide, Australia.

Stevens, K. N. (2000). *Acoustic phonetics*, Vol. 30, MIT Press, London.